

Bulk and surface electronic structures of MgO

U. Schönberger

*Max-Planck-Institut für Metallforschung, Institut für Werkstoffwissenschaft,
Seestrasse 92, 70174 Stuttgart, Federal Republic of Germany*

F. Aryasetiawan

Max-Planck-Institut für Festkörperforschung, Heisenbergstrasse 1, 70569 Stuttgart, Federal Republic of Germany

(Received 21 February 1995)

The bulk electronic structure of MgO is calculated from first principles including correlation effects within the *GW* approximation. The band gap, the position of the *2s* O band, and the valence band width are in good agreement with experiment. From the quasiparticle band structure, optical transitions corresponding to the main optical absorption peaks are identified. The energy-loss spectrum is also calculated and compared with experiment. The surface electronic structure of MgO(100) is calculated self-consistently within the local-density approximation. It is found that states observed in a recent photoemission experiment outside the bulk allowed states are close to surface states.

I. INTRODUCTION

The electronic structure of MgO with sodium chloride structure has been the subject of many studies¹⁻¹³ because it is a prototype for simple oxides. From a technological point of view, it is an important material with many applications. Most of the band-structure calculations have been based on the local-density approximation (LDA) within the density-functional theory.¹⁴ It is well known that a comparison between the single-particle eigenvalues in the LDA with the experimental photoemission band structure is not warranted by the theory. Nevertheless, for simple *sp* systems such as MgO, the LDA valence band structures are often in good agreement with experiment. However, there are problems due to the neglect of the nonlocality and energy dependence in the exchange-correlation potential. The band gap of MgO in the LDA is ~ 5 eV whereas experimentally it is ~ 8 eV.^{15,16} This appears to be quite a general problem in the LDA. The problem becomes worse in the transition metal oxides where the LDA in some cases gives a wrong prediction for the ground state. For example, the LDA predicts FeO, CoO, and CuO to be metals whereas experimentally, they are insulators.

One of the objectives of this paper is to study the bulk electronic structure of MgO including correlation effects. We have performed a first-principles calculation of the quasiparticle band structure within the *GW* approximation (GWA).¹⁷⁻¹⁹ From the quasiparticle band structure, we identify the main optical transitions corresponding to the main peaks in the experimental optical absorption spectra. There have been considerable differences in the assignment of these optical transitions in the literature. Furthermore, as a measure of the quality of the screened Coulomb potential used in the GWA, we have calculated the energy-loss spectra and made comparison with ex-

periment.

Another objective of this paper is motivated by a recent angle-resolved photoemission measurement on MgO,²⁸ that reveals the existence of some states that appear to lie outside the bulk bands. The origin of these states is ambiguous. For this reason, we have performed a self-consistent first-principles calculation of the surface electronic structure in order to clarify the origin of these states. The calculation has been performed within the LDA. Inclusion of the self-energy correction is at the present stage not feasible due to the large computational size. However, our results for the bulk band structure within the GWA indicate that the valence band structure is well described by the LDA. In addition, we have also investigated a possible atomic rumpling that has been proposed in the literature.

II. THEORY AND NUMERICAL METHOD

The self-energy within the GWA is given by^{17,18}

$$\Sigma(\mathbf{r}, \mathbf{r}'; \omega) = \frac{i}{2\pi} \int d\omega' G(\mathbf{r}, \mathbf{r}'; \omega + \omega') W(\mathbf{r}, \mathbf{r}'; \omega'). \quad (1)$$

In practice, the self-consistent Green function G is replaced by a zeroth-order Green function G_0 , which in our case is constructed from the LDA Bloch states. The screened potential W is given by

$$W(\mathbf{r}, \mathbf{r}'; \omega) = \int d^3r'' \epsilon^{-1}(\mathbf{r}, \mathbf{r}''; \omega) v(\mathbf{r}'' - \mathbf{r}'), \quad (2)$$

where ϵ^{-1} is the inverse dielectric matrix and v is the bare Coulomb potential. A method for calculating ϵ^{-1} is described in detail in a previous publication.²⁰ The method can be used also for systems containing d and f

electrons. For the LDA band-structure calculations, we use the linear muffin-tin orbital²¹ (LMTO) method. The LMTO basis within the atomic sphere approximation²¹ (ASA) has the following form:

$$\chi_{\mathbf{R}\mathbf{L}} = \phi_{\mathbf{R}\mathbf{L}} + \sum_{\mathbf{R}'\mathbf{L}'} \dot{\phi}_{\mathbf{R}'\mathbf{L}'} h_{\mathbf{R}'\mathbf{L}',\mathbf{R}\mathbf{L}}, \quad (3)$$

where $\mathbf{R}\mathbf{L}$ denotes the site and angular momentum (l, m), respectively, ϕ is the solution to the Schrödinger equation inside the muffin-tin sphere, and $\dot{\phi}$ is its energy derivative taken at some fixed energy ϵ_ν . The response function within the random phase approximation²² (RPA) consists of products of Bloch states so that the Hilbert space spanned by the response function is formed by products of the type $\phi\phi$, $\phi\dot{\phi}$, and $\dot{\phi}\dot{\phi}$. Some of these products are linearly dependent and we construct an optimized basis for ϵ^{-1} by forming linear combinations of these product functions and throwing away linearly dependent combinations. The number of basis functions per atom is typically 50–100.²⁰ The total number of basis functions used in our present calculation is 125.

The quasiparticle energies are obtained in a standard way as follows:¹⁹

$$E_{\mathbf{k}n} = \epsilon_{\mathbf{k}n} + Z_{\mathbf{k}n} \Delta\Sigma(\epsilon_{\mathbf{k}n}), \quad (4)$$

where $\epsilon_{\mathbf{k}n}$ is the LDA eigenvalue and

$$\Delta\Sigma(\epsilon_{\mathbf{k}n}) = \langle \psi_{\mathbf{k}n} | \Sigma(\epsilon_{\mathbf{k}n}) - v_{xc}^{\text{LDA}} | \psi_{\mathbf{k}n} \rangle. \quad (5)$$

The Z factor, which is the weight of the quasiparticle, is given by

$$Z_{\mathbf{k}n} = \left[1 - \frac{\partial \Sigma(\epsilon_{\mathbf{k}n})}{\partial \omega} \right]^{-1} < 1. \quad (6)$$

The energy-loss spectra is given by

$$\text{ELS}(\mathbf{q}, \omega) = -\text{Im} \epsilon^{-1}(\mathbf{q}, \omega), \quad (7)$$

where $\epsilon^{-1}(\mathbf{q}, \omega)$ is the Fourier transform of $\epsilon^{-1}(\mathbf{r}, \mathbf{r}'; \omega)$. In our calculation, we include the effects of local field that are usually neglected in most calculations. The MgO(001) surface calculations have been performed within the LDA with a repeated slab geometry. For solving the one-particle Schrödinger equation we applied a full-potential LMTO method.²³ The use of nonoverlapping spheres increases the number of basis functions compared to the LMTO-ASA method. In the interstitial region the products of LMTO's have been expanded in a set of Hankel functions fitted to the value and the first derivative on the sphere surfaces. More details about this method may be found in the work of Methfessel, Hennig, and Scheffler,²⁴ where they calculated the low-index $4d$ transition metal surfaces. For the calculation of possible atomic relaxations at the MgO surface it has turned out to be essential to have no shape approximation on the charge density and the potential. The exchange and correlation potential of Hedin and Lundqvist²⁵ was used. The basis set consists of 2(Mg $3s$), 2(Mg $3p$), 2(O $2s$), and 2(O $2p$) functions with kinetic energies of $-\kappa^2 = -0.7$

and -1.0 Ry, which leads to 8 basis functions per atom. The band structures have been calculated with the same muffin-tin radii for O and Mg, which are 0.7% smaller than the touching and the experimental lattice constant ($a_{\text{exp}} = 4.21$ Å). The disappearance of surface band splittings with 9 layers indicates slab size convergence.

The calculation of surface relaxation was done with a five-layer slab and with spheres 1.5% smaller than the touching and the theoretical predicted bulk lattice constant ($a_{\text{theo}} = 4.16$ Å). Empty spheres between the MgO layers and one layer of empty spheres on top of the surface were introduced to have a better representation of the charge density in the interstitial region. The tails of the Hankel functions were augmented up to $l = 4$. The charge density was expanded within the spheres up to $l = 4$, except for the surface empty spheres where the expansion was done up to $l = 6$. The \mathbf{k} -space integration was performed with a sampling technique²⁶ with 2 and 4 divisions in the perpendicular direction to the surface and up to 12 divisions in the parallel directions (up to 72 irreducible points).

III. RESULTS AND DISCUSSIONS

A. Bulk electronic structure

The LDA band structure along ΓX and ΓL is shown in Fig. 1. The band structure is calculated with the LMTO-ASA method. It is in good agreement with the band structure calculated using a full-potential LMTO. The LDA band gap is 5.2 eV and it is a direct gap at the Γ point. The large gap is as expected because MgO is highly ionic. Comparison with other calculations is given in Table I.

The values vary from 4.2 to 8.9 eV and our value is closest to the value obtained with the linear-augmented-plane-wave (LAPW) method.⁹ The LDA band gap is too small compared with the experimental optical band gap

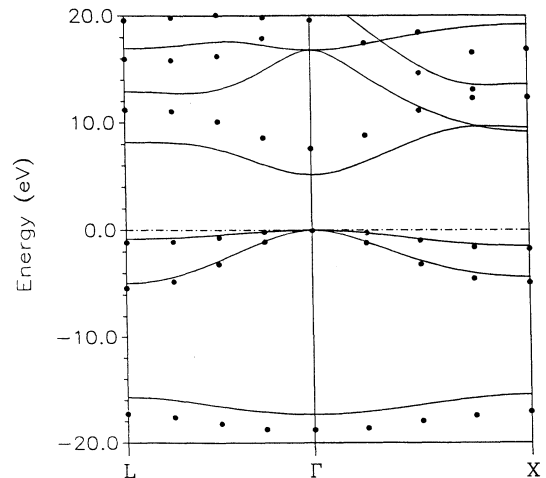


FIG. 1. Energy bands of MgO from LMTO-ASA (solid line) and GWA (dots) calculations.

[7.8 eV (Ref. 16)]. The width of the upper valence band is 4.9 eV, which is in good agreement with the experimental values (5 – 6 eV). The position of the top of the low-lying oxygen *s* band in the LDA is at 15.5 eV and the experimental values lie between 18 and 21 eV.

In Fig. 2 we show the total and partial density of states. The top of the valence band is primarily O *p* and the bottom of the conduction band is Mg *s*. As can be seen from the partial density of states, there is a large hybridization between Mg and O in both the valence and conduction bands. In Fig. 1 we show the *GW* quasiparticle band structure. The *GW* band gap is found to be 7.7 eV, which is in good agreement with the experimental value of 7.8 eV. The experimental gap corresponds to the optical gap whereas our theoretical gap should be compared to the photoemission gap, which is smaller because it contains no excitonic effects. Assuming the *GW* gap is close to the correct gap, we expect the excitonic binding energy to be small.

TABLE I. The band gap of MgO determined by different methods.

| Method | gap (eV) |
|-------------------------------------------------------------------------|----------|
| Experiment ^a | 7.83 |
| GWA ^b | 7.7 |
| LMTO-ASA ^c (LDA) | 5.2 |
| Full-potential LMTO ^d (LDA) | 5.0 |
| LAPW ^e (LDA) | 4.98 |
| LMTO-ASA ^f (LDA) | 6.06 |
| Orthogonalized linear combination of atomic orbitals ^g (LDA) | 4.19 |
| Pseudopotential ^h (<i>pp</i>) (LDA) | 4.5 |
| <i>pp</i> mixed basis ⁱ (LDA) | 4.36 |
| Augmented plane wave ^j (LDA) | 4.65 |
| Pseudofunction ^k (LDA) | 4.63 |
| Korringa-Kohn-Rostoker ^l | 5.37 |
| Hartree-Fock ^m | 8.9 |
| Hartree-Fock + corr. ⁿ | 8.21 |
| Hartree-Fock-Slater ^o | 7.53 |
| Tight-binding ^p | 7.76 |
| Empirical <i>pp</i> ^q | 7.77 |

^aWhited, Flaten, and Walker, 1973 (Ref. 16).

^bOur calculation.

^cOur calculation.

^dOur calculation.

^eStepanyuk *et al.*, 1989 (Ref. 9).

^fTaurian, Springborg, and Christensen, 1985 (Ref. 7). The inclusion of “empty spheres” leads to a gap of ≈ 5.0 eV (see Note in Ref. 8).

^gXu and Ching, 1991 (Ref. 12).

^hChang and Cohen, 1984 (Ref. 6).

ⁱWang and Holzwarth, 1990 (Ref. 11).

^jKlein *et al.*, 1987 (Ref. 8).

^kBortz *et al.*, 1990 (Ref. 10).

^lYamashita and Asano, 1970 (Ref. 2).

^mPantelides, Mickish, and Kunz, 1974 (Ref. 4).

ⁿPandey, Jaffe, and Kunz, 1991 (Ref. 13).

^oWalch and Ellis, 1973 (Ref. 3).

^pDaude, Jouanin, and Gout, 1977 (Ref. 5).

^qFong, Saslow, and Cohen, 1968 (Ref. 1).

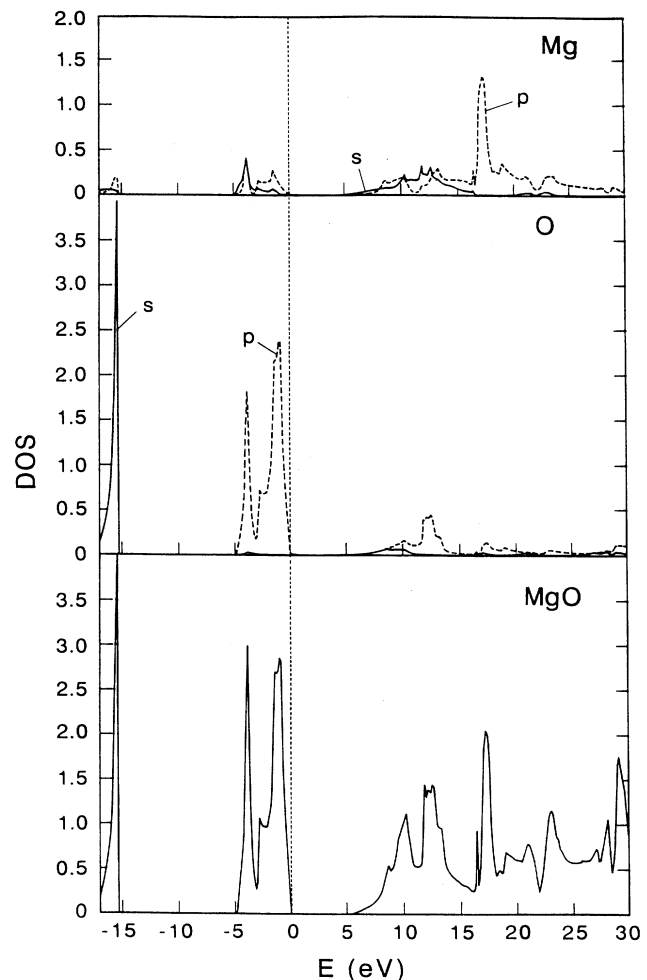


FIG. 2. Total density of states (DOS) of MgO (lower panel) and partial DOS of O (middle panel) and Mg (upper panel).

The result for the band gap can perhaps be understood if we regard the GWA as a Hartree-Fock approximation (HFA) with dynamically screened Coulomb potential. In the HFA, the band gap is overestimated and the RPA screening reduces the gap to the correct value. For *s-p* systems such as MgO, the screening is expected to be dominated by the long-range Coulomb correlation, which is well described by the RPA.

The self-energy correction lowers the O *2s* band by ~ 2 eV so that the top of the band lies at 18 eV, which is rather close to the experimental values (18–21 eV). It is known that the LDA places core or corelike states too high, which may be understood by the presence of self-interaction, which is absent in the GWA, thereby lowering the O *2s* band.

From Fig. 1, it can be seen that the self-energy correction is almost independent of the *k* point. The valence band is essentially unchanged from the LDA result, except for a small increase of 0.3 eV in the band width. These results are qualitatively similar to those for semiconductors where the correct result is also sim-

TABLE II. The main characters of the states at high symmetry points.

| State | ϵ_{kn} (eV) | Mg | O |
|----------------|----------------------|--------------|--------------|
| Γ_{15} | 0.0 | 7% <i>p</i> | 93% <i>p</i> |
| Γ_1 | 5.2 | 50% <i>s</i> | 20% <i>s</i> |
| Γ'_{25} | 15.7 | 70% <i>d</i> | 15% <i>d</i> |
| X'_4 | -4.3 | 30% <i>p</i> | 60% <i>p</i> |
| X'_5 | -1.5 | 16% <i>p</i> | 80% <i>p</i> |
| X_3 | 9.0 | 54% <i>d</i> | 11% <i>d</i> |
| X_1 | 9.6 | 73% <i>s</i> | 11% <i>d</i> |
| X_5 | 13.7 | 30% <i>p</i> | 36% <i>p</i> |
| L_2 | -4.9 | 30% <i>s</i> | 60% <i>p</i> |
| L_3 | -0.8 | 15% <i>d</i> | 85% <i>p</i> |
| L'_2 | 8.1 | 51% <i>p</i> | 10% <i>s</i> |
| | | | 6% <i>d</i> |
| L'_3 | 12.9 | 23% <i>s</i> | 40% <i>p</i> |
| | | 6% <i>d</i> | |
| L_1 | 16.4 | 70% <i>p</i> | 16% <i>d</i> |

ply obtained by a rigid shift of the LDA conduction band, which is called scissor operator in the literature.

Optical absorption measurements on MgO reveal prominent peaks at 7.7, 10.8, 13.3, and 16.8 eV. Due to differences in the calculated conduction band structure, there have been considerable differences in the assignment of which transitions leading to these main peaks. With the proper inclusion of correlation effects in the band structure, a reliable assignment can be made. To find out which transitions are allowed, we list in Table II the main characters of the states at the high symmetry points Γ , X , and L . In Table III we deduce from the *GW* quasiparticle band structure, the transitions which are expected to correspond to the main peaks in the experimental optical absorption.

The peak at 7.7 eV is probably predominantly excitonic because from Table II, the main character of the highest valence state at the Γ point is O *p*, whereas the lowest conduction state is Mg *s* resulting in small optical transitions. Comparison with previous works in Table III reveals that our assignment for each peak agrees with at least two other works.

We have also calculated the energy-loss spectrum of MgO within the RPA. The result is shown in Fig. 3 together with the experimental result.²⁷ The peak at ~ 24 eV is a plasmon peak that is very close to the plasmon energy estimated from the electron gas formula $\omega_p = \sqrt{4\pi\rho}$. The structures below and above the plasmon

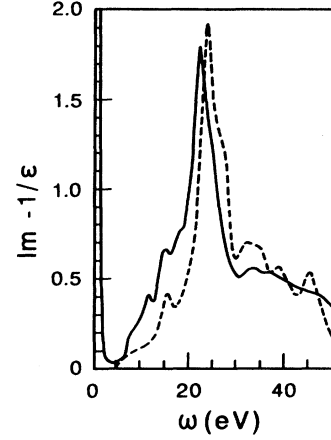


FIG. 3. Calculated (broken line) and measured energy-loss spectrum (Ref. 26) (full line).

energy are evidently due to the band structure, which are also observed experimentally. The calculation is performed with only *s*, *p* and *d* orbitals and it takes into account local field effects but they are found to be almost negligible. We note that that spectrum was calculated for $\mathbf{q} = (0.25, 0, 0)2\pi/a$ whereas the experimental spectrum corresponds to $\mathbf{q} = 0$. This explains the shift towards higher energy of the theoretical spectrum with respect to the experiment. Since the energy-loss spectrum is proportional to the imaginary part of the screened Coulomb potential ($\text{Im}W$) for long wavelength, the reasonable agreement with experiment shows that the long-range screening is well described by the RPA and it provides a good input for the *GW* calculation.

B. Surface electronic structure

In a recent experiment the electronic structure of MgO was studied by Tjeng, Vos, and Sawatzky²⁸ with angle-resolved ultraviolet photoelectron spectroscopy. The band structure of MgO along a circular path in the ΓXWK and the ΓXUL plane have been measured. Since band-structure calculations are only available in the literature along high symmetry lines, the band structure along the circular path has been calculated by Tjeng, Vos, and Sawatzky with a bulk fitted tight-binding model. The overall agreement with experiment turns out to be

TABLE III. Prominent peak positions in the optical absorption and their assignment.

| Peak position (eV) | <i>GW</i> | HF+correlation | LDA pseudofunction | Empirical pseudopotential |
|--------------------|------------------------|------------------------|------------------------|---------------------------|
| Ref. 15 | Our calculation | Ref. 13 | Ref. 10 | method Ref. 1 |
| 7.7 | $\Gamma_{15}-\Gamma_1$ | $\Gamma_{15}-\Gamma_1$ | $\Gamma_{15}-\Gamma_1$ | $\Gamma_{15}-\Gamma_1$ |
| 10.8 | $L_3-L'_2$ | $L_3-L'_2$ | X'_5-X_1 | $L_3-L'_2$ |
| 13.3 | X'_5-X_1, X_3 | X'_5-X_3 | X'_5-X_3 | $\Sigma_4-\Sigma_1$ |
| 16.8 | X'_4-X_1, X_3 | X'_5-X_1 | X'_4-X_3 | X'_4-X_3 |
| | $L_2-L'_2$ | | | |

very good. However, additional peaks, ~ 0.9 eV lower than the valence band top,²⁹ were found in the ΓXWK plane, which cannot be explained by the tight-binding bands. As one possible explanation, angle-integrated transitions were proposed. On the other hand, these peaks fall outside the bulk allowed states at the \bar{M} point of the surface Brillouin zone and a possible attribution to surface states could not be excluded.

The band structure of the MgO (100) and (110) surface was previously calculated by Lee and Wong with a bulk fitted tight-binding model.³⁰ Most of the surface bands in this calculation could be explained by the reduction of the Madelung energy at the surface. This reduction, however, enters in the calculation as a parameter. To have a better understanding for the origin of these states, we have performed self-consistent *ab initio* surface calculations. The results for the MgO(100) surface band structure along $\bar{\Gamma}-\bar{M}-\bar{X}-\bar{\Gamma}$ are shown in Fig. 4 and compared with the tight-binding band structure. In addition, the experimental peaks are included relative to the local valence band top at \bar{M} , which are nearly coincident with one surface band. One has to note that the experimental peaks have been measured on a circular path, which is near the $\bar{\Gamma}-\bar{M}$ line but that dispersion along the projection path is ignored. Surface resonances in the bulk allowed regions have not been analyzed in our study yet. Since the valence band width and the band gap differ in both calculations not all the surface bands found by Lee and Wong are included in Fig. 4. We expect the surface relaxation to be very small and used the undistorted surface structure for the calculations of the band structure. This has been supported by a recent theoretical study by Pugh and Gillan,³² who found the relaxation effects to be exceedingly small. Our total-energy calculation shows that a "rumpling" at the surface, which has been observed experimentally by a low-energy electron diffraction measurement³¹ is energetically unfavorable by 0.02 eV per MgO.

The continuum of the bulk projected band structure (hatched area) has been constructed by folding down the calculated bulk band structure to the surface Brillouin zone.

In three regions outside the bulk band-structure surface states are found in both studies. Firstly, one surface band appears below the bottom of the bulk conduction band reducing the band gap by about 0.6 eV. The finding of the more localized surface band in the previous tight-binding study could not be supported. Secondly, there is a flat surface band on top of the bulk conduction band. We found no surface band creating an indirect gap near the \bar{X} point like in the study of Lee and Wong. Moreover, one surface band instead of two (which have not been included in Fig. 4) appears in the relative gap of the valence states near the \bar{X} point. Most of the differences described above may be attributed to self-consistency and the more complete basis set of our treatment.

The lowest unoccupied surface band with mostly Mg *s* character has very similar dispersion as the bottom of the bulk conduction band. One can explain its appearance qualitatively by simple electrostatic arguments, namely,

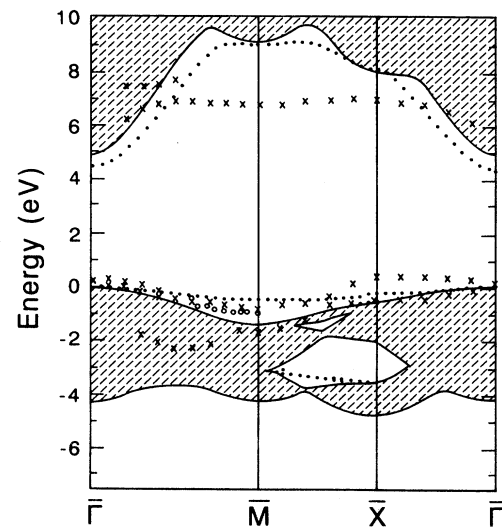


FIG. 4. Surface band structure of MgO(100) (dots). The experimental result of Tjeng, Vos, and Sawatzky (Ref. 28) (open dots) and the theoretical result of Lee and Wong (Ref. 30) (crosses) have been added.

the reduction of the Madelung energy at the surface proposed by Levine and Mark.³³ To what extent this holds for the highest occupied surface band and how much its dispersion reflects charge redistribution at the surface might be analyzed from our result by model calculations.

IV. SUMMARY AND CONCLUSIONS

We have calculated from first principles the bulk band structure of MgO including the effects of correlation. The band gap and the position of the semicore O *2s* are in good agreement with experiment and the self-energy correction has little effect on the LDA valence band. We expect therefore that the same is true in the surface case except for the unoccupied bands, which should be shifted up if self-energy correction is included. The LDA surface calculations have been performed self-consistently. We compare the surface band structure with experiment and with an earlier calculation based on a tight-binding model. It is found that the recently observed nonbulk states in photoemission experiments can be attributed to surface states. We have also investigated the possible rumpling but found that it is energetically unfavorable by 0.02 eV.

ACKNOWLEDGMENTS

We would like to thank Dr. C. Arcangeli for help in performing the energy-loss spectrum and Dr. M. Methfessel for continuous assistance of the full-potential LMTO calculations. This work has been supported in part by the European Community program Human Capital and Mobility through Contract No. CHR-CT93-0337.

- ¹ C. Y. Fong, W. Saslow, and M. L. Cohen, *Phys. Rev.* **168**, 992 (1968).
- ² J. Yamashita and S. Asano, *J. Phys. Soc. Jpn.* **28**, 1143 (1970).
- ³ P. F. Walch and D. E. Ellis, *Phys. Rev. B* **8**, 5920 (1973).
- ⁴ S. T. Pantelides, D. J. Mickish, and A. B. Kunz, *Phys. Rev. B* **10**, 5203 (1974).
- ⁵ N. Daude, C. Jouanin, and C. Gout, *Phys. Rev. B* **15**, 2399 (1977).
- ⁶ K. J. Chang and M. L. Cohen, *Phys. Rev. B* **30**, 4774 (1984).
- ⁷ O. E. Taurian, M. Springborg, and N. E. Christensen, *Solid State Commun.* **55**, 351 (1985).
- ⁸ Barry M. Klein, Warren E. Pickett, Larry L. Boyer, and R. Zeller, *Phys. Rev. B* **35**, 5802 (1987).
- ⁹ V. S. Stepanyuk, A. Szasz, B. L. Grigorenko, O. V. Farberovich, and A. A. Katsnelson, *Phys. Status Solidi B* **155**, 179 (1989).
- ¹⁰ M. L. Bortz, R. H. French, D. J. Jones, R. V. Kasowski, and F. S. Ohuchi, *Phys. Scr.* **41**, 537 (1990).
- ¹¹ Q. S. Wang and N. A. W. Holzwarth, *Phys. Rev. B* **41**, 3211 (1990).
- ¹² Y-N Xu and W. Y. Ching, *Phys. Rev. B* **43**, 4461 (1991).
- ¹³ R. Pandey, J. E. Jaffe, and A. B. Kunz, *Phys. Rev. B* **43**, 9228 (1991).
- ¹⁴ P. Hohenberg and W. Kohn, *Phys. Rev.* **136**, B864 (1964); W. Kohn and L.J. Sham, *Phys. Rev.* **140**, A1133 (1965).
- ¹⁵ D. M. Roessler and W. C. Walker, *Phys. Rev.* **159**, 733 (1967).
- ¹⁶ R. C. Whited, C. J. Flaten, and W. C. Walker, *Solid State Commun.* **13**, 1903 (1973).
- ¹⁷ L. Hedin, *Phys. Rev.* **139**, A796 (1965).
- ¹⁸ L. Hedin and S. Lundqvist, in *Solid State Physics*, edited by H. Ehrenreich, F. Seitz, and D. Turnbull (Academic, New York, 1969), Vol. 23, p. 1.
- ¹⁹ F. Aryasetiawan, *Phys. Rev. B* **46**, 13 051 (1992).
- ²⁰ F. Aryasetiawan and O. Gunnarsson, *Phys. Rev. B* **49**, 16 214 (1994).
- ²¹ O.K. Andersen, *Phys. Rev. B* **12**, 3060 (1975).
- ²² D. Pines, *Elementary Excitations in Solids* (Benjamin, New York, 1963).
- ²³ M. Methfessel, *Phys. Rev. B* **38**, 1537 (1988).
- ²⁴ M. Methfessel, D. Hennig, and M. Scheffler, *Phys. Rev. B* **46**, 4816 (1992).
- ²⁵ L. Hedin and B. I. Lundqvist, *J. Phys.* **4**, 2064 (1971).
- ²⁶ M. Methfessel and A. T. Paxton, *Phys. Rev. B* **40**, 3616 (1989).
- ²⁷ C. C. Ahn and O. L. Krivanek, *EELS Atlas(HREM facility)* (Arizona State University, Tempe, 1983).
- ²⁸ L. H. Tjeng, A. R. Vos, and G. A. Sawatzky, *Surf. Sci.* **235**, 269 (1990).
- ²⁹ We calculated this circular path of bulk band structure within the $\Gamma X W K$ plane with our method. The result is in very good agreement to the result calculated in Ref. 28.
- ³⁰ Ven-Chung Lee and How-Sen Wong, *J. Phys. Soc. Jpn.* **45**, 895 (1978).
- ³¹ M. R. Welton-Cook and W. Berndt, *J. Phys. C* **15**, 5691 (1982).
- ³² S. Pugh and M. J. Gillan, *Surf. Sci.* **320**, 331 (1994).
- ³³ J. D. Levine and P. Mark, *Phys. Rev.* **144**, 751 (1966).